Two fluid equation considering time-dependent change of thermal-hydraulic volume

Jong Hyuk Lee [a*], Byoung Jae Kim[b], Kyung Doo Kim [a]
[a]*Thermal Hydraulics and Severe Accident Division, Korea Atomic Energy Research Institute, 989-111 Daedeok-daero, Yuseong-gu, Daejeon, 34057kns, Rep. of Korea.*
[b]*School of Mechanical Engineering, Chungnam National University, 99 Daehak-ro, Yuseong-gu, Daejeon, 34134, Rep. of Korea.*
[*]*Corresponding author: leejonghyuk@kaeri.re.kr*

1. Introduction

When a core in nuclear reactor is uncovered due to accidents like as large-break loss of coolant accident (LBLOCA), the fuel cladding can be deformed by an internal pressure rise of fuel due to overheating. The deformation of fuel cladding cause the change of flow area and, the coolability of core flow can be affected by the flow redistribution. And, the U.S Nuclear Regulatory Commission (NRC) issued a revision to 10CFR50.46c which contain calculated changes in core geometry shall be the core remains amenable to cooling. Therefore, it is important to expect thermal-hydraulics phenomena according to the change of flow path in a core.

The purpose of this study is to establish the governing equations considering the change of flow path and verify the capability of the SPACE code. In order to consider the change of flow path with time, a fluid porosity is applied into two-fluid equations. Two fluid equations with time-dependent porosity are derived and a conceptual problem having a change of flow path was simulated for a single flow.

2. Two fluid equation with time-dependent fluid porosity

2.1 Continuity equation

One-dimensional conservative equation is considered in this study.

$$\frac{\partial}{\partial t}(\varepsilon\alpha_k\bar{\bar{\rho}}_k)+\nabla\cdot(\varepsilon\alpha_k\bar{\bar{\rho}}_k\widehat{\mathbf{u}_k})=\varepsilon\Gamma_{ik} \tag{1}$$

Based on the code structure of SPACE code, continuity equation of gas, liquid, droplet, and non-condensable (NC) gas phase is as follows:

$$\frac{\partial}{\partial t}(\varepsilon\alpha_g\rho_v)+\nabla\cdot(\varepsilon\alpha_g\rho_v\mathbf{u}_g)=\varepsilon(\Gamma_l+\Gamma_d+\Gamma_l^w+\Gamma_d^w) \tag{2}$$

$$\frac{\partial}{\partial t}(\varepsilon\alpha_l\rho_l)+\nabla\cdot(\varepsilon\alpha_l\rho_l\mathbf{u}_l)=\varepsilon(-\Gamma_l-S_E+S_D-\Gamma_l^w) \tag{3}$$

$$\frac{\partial}{\partial t}(\varepsilon\alpha_d\rho_d)+\nabla\cdot(\varepsilon\alpha_d\rho_d\mathbf{u}_d)=\varepsilon(-\Gamma_d+S_E-S_D-\Gamma_d^w) \tag{4}$$

$$\frac{\partial}{\partial t}(\varepsilon\alpha_g\rho_n)+\nabla\cdot(\varepsilon\alpha_g\rho_n\mathbf{u}_g)=0 \tag{5}$$

Where *v*, *l*, *d*, *g*, and *n* is vapor, liquid, droplet, gas, and NC gas. Γ_l and Γ_d is the amount of evaporation from liquid interface and droplet interface.

2.2 Conservation of energy (internal)

The balance of energy can be written by considering the internal energy of the fluid. Thus local equation is

$$\frac{\partial}{\partial t}(\rho_k e_k)+\nabla\cdot(\rho_k e_k\mathbf{u}_k)=-\nabla\cdot\mathbf{q}_k-p_k\nabla\cdot\mathbf{u}_k+\Phi_k \tag{6}$$

The above equation is integrated by a control volume of k-phase(V_K), and divided by a total volume(V). Then we have:

$$\begin{aligned}&\frac{1}{V}\int_{V_k}\frac{\partial}{\partial t}(\rho_k e_k)dV+\frac{1}{V}\int_{V_k}\nabla\cdot(\rho_k e_k\mathbf{u}_k)dV\\&=-\frac{1}{V}\int_{V_k}\nabla\cdot\mathbf{q}_k dV-\frac{1}{V}\int_{V_k}p_k\nabla\cdot\mathbf{u}_k dV+\frac{1}{V}\int_{V_k}\Phi_k dV\end{aligned} \tag{7}$$

The Eq.(7) can be summarized using divergence, averaging and Leibnitz theorem as below:

$$\begin{aligned}&\frac{\partial}{\partial t}(\varepsilon\alpha_k\bar{\bar{\rho}}_k\widehat{e_k})+\nabla\cdot(\varepsilon\alpha_k\bar{\bar{\rho}}_k\widehat{e_k}\widehat{\mathbf{u}_k})\\&=-\nabla\cdot[\varepsilon\alpha_k(\bar{\bar{\mathbf{q}}}_k+\mathbf{q}_k^{\mathrm{Re},e})]+\varepsilon Q_{ik}+\varepsilon Q_{sk}\\&-\bar{\bar{p}}_k\nabla\cdot(\varepsilon\alpha_k\bar{\bar{\mathbf{u}}}_k)+\varepsilon\Gamma_{ik}\hat{h}_{ik}-\bar{\bar{p}}_k\frac{\partial}{\partial t}(\varepsilon\alpha_k)+\varepsilon\alpha_k\bar{\bar{\Phi}}_k\end{aligned} \tag{8}$$

Where, $\hat{h}_{ik}\equiv\bar{\bar{p}}_k/\hat{\rho}_{ik}+\hat{e}_{ik}$

For one dimensional flow, the terms including $\bar{\bar{q}}_k$ and $q_k^{\mathrm{Re},\varepsilon}$ are able to be negligible because the velocity and temperature in is almost constant at the fluid cross-section,

Finally, we obtain

$$\begin{aligned}&\frac{\partial}{\partial t}(\varepsilon\alpha_k\bar{\bar{\rho}}_k\widehat{e_k})+\frac{\partial}{\partial x}(\varepsilon\alpha_k\bar{\bar{\rho}}_k\widehat{e_k}\widehat{u_k})=-\bar{\bar{p}}_k\frac{\partial}{\partial t}(\varepsilon\alpha_k)\\&-\bar{\bar{p}}_k\nabla\cdot(\varepsilon\alpha_k\bar{\bar{u}}_k)+\varepsilon(Q_{ik}+Q_{sk}+\Gamma_{ik}\hat{h}_{ik}+\alpha_k\bar{\bar{\Phi}}_k)\end{aligned} \tag{9}$$

2.3 Conservation of momentum

We take the conservation of momentum below:

$$\begin{aligned}&\frac{\partial}{\partial t}(\varepsilon\alpha_k\bar{\bar{\rho}}_k\widehat{\mathbf{u}_k})+\nabla\cdot(\varepsilon\alpha_k\bar{\bar{\rho}}_k\widehat{\psi_k}\widehat{\mathbf{u}_k})\\&=-\nabla(\varepsilon\alpha_k\bar{\bar{p}}_k)+\nabla\cdot(\varepsilon\alpha_k\bar{\bar{\boldsymbol{\tau}}}_k)+\nabla\cdot(\varepsilon\alpha_k\boldsymbol{\tau}_k^{\mathrm{Re}})\\&+\varepsilon\Gamma_{ik}\hat{\mathbf{u}}_{ik}+\varepsilon\alpha_k\bar{\bar{\rho}}_k\mathbf{g}-\frac{1}{V}\int_{A_{k,i}}(p_k\mathbf{I}-\boldsymbol{\tau}_k)\cdot\mathbf{n}_k dA\\&-\frac{1}{V}\int_{A_{k,s}}(p_k\mathbf{I}-\boldsymbol{\tau}_k)\cdot\mathbf{n}_k dA\end{aligned}\quad(10)$$

Based on Prosperetii[1], the friction term was proposed as:

$$\mathbf{F}_{ik}\equiv\frac{1}{V}\int_{A_{k,i}}[-(p_k-\bar{\bar{p}}_k)\mathbf{I}+(\boldsymbol{\tau}_k-\bar{\bar{\boldsymbol{\tau}}}_k)\cdot\mathbf{n}_k]dA=\varepsilon f_{ik}$$

$$\mathbf{F}_{sk}=\varepsilon f_{sk}$$

Using the averaging theorem, Eq. (10) can be summarized as below if we have non-conservative momentum equation.

$$\begin{aligned}&\varepsilon\alpha_k\bar{\bar{\rho}}_k\left(\frac{\partial\widehat{u_k}}{\partial t}+\widehat{u_k}\frac{\partial\widehat{u_k}}{\partial x}\right)=-\varepsilon\alpha_k\frac{\partial\bar{\bar{p}}_k}{\partial x}\\&+\varepsilon\Gamma_{ki}(\hat{u}_{ik}-\widehat{u_k})+\varepsilon f_{ik}+\varepsilon f_{sk}+\varepsilon\alpha_k\bar{\bar{\rho}}_k g_x\end{aligned}\quad(11)$$

Divided by porosity (ε),

$$\begin{aligned}&\alpha_k\bar{\bar{\rho}}_k\left(\frac{\partial\widehat{u_k}}{\partial t}+\widehat{u_k}\frac{\partial\widehat{u_k}}{\partial x}\right)=-\alpha_k\frac{\partial\bar{\bar{p}}_k}{\partial x}\\&+\Gamma_{ki}(\hat{u}_{ik}-\widehat{u_k})+f_{ik}+f_{sk}+\alpha_k\bar{\bar{\rho}}_k g_x\end{aligned}\quad(12)$$

3. Verification

The two-equation with time-dependent porosity, which finally derived Eq. (1), (9) and (12), were employed into the SPACE code. A conceptual problem with a simple geometry was used to verify SPACE code including the derived equations for a single-phase liquid flow

A conceptual problem was introduced to verify the SPACE code. A single pipe with a 0.1 m of diameter and 3.6 m of height was initially set. The water, constantly injected at 0.1 m/s, flows into the pipe from downside to upside under non-heating condition.

Fig 1 shows the nodalization of SPACE code for the vertical pipe. We assumed that the three cells from 10th to 12th (C115) started to change the porosity at certain time and the change of the cells have finished within one second. The value of target porosity is set as 0.2 and the change rate of porosity also considered.

The comparisons of velocity and mass flow rate for the cases between the unchanged and the changed flow path represented in Fig 2. Those are compared at three positions: Upstream (3rd cell from the inlet), Changed part (10, 11 and 12th cell) and Downstream (17th cell from the inlet or 3rd cell before the outlet).

For the no change of flow path, the velocity and mass flow rate is a constant. However, velocity at changed cells increased by decreasing the flow area. Passing through the changed part, the velocity is the same as the one at the upstream.

A mass balance from inlet to outlet is always conserved even if flow path at a certain height is changed. Fig 3 shows the comparison of mass error for the changed flow path with the unchanged one. Mass error is defined in this paper as:

$$\text{mass error (-)}=\frac{(\sum m_{\text{cell,initial}}+m_{\text{in}}-m_{\text{out}})-\sum m_{\text{cell}}}{\sum m_{\text{cell,initial}}}$$

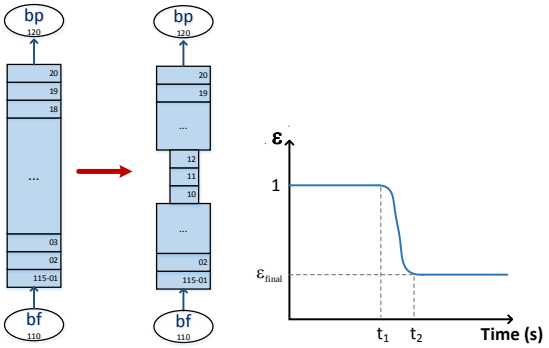

Fig. 1 Node diagram and the change rate of porosity for conceptual problem

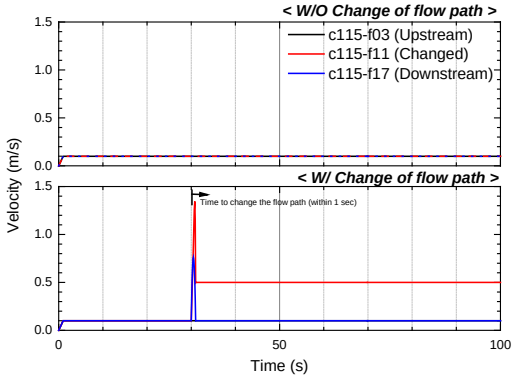

(a) velocity

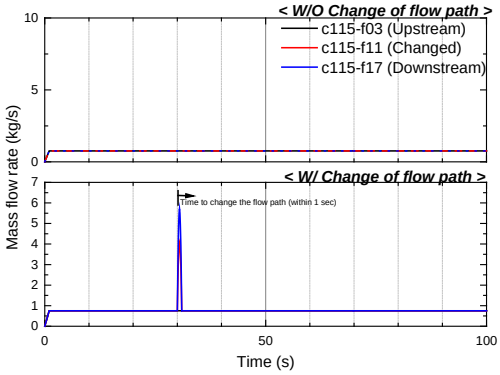

(b) Mass flow rate

Fig. 2 Comparisons of velocity and mass flow rate at each location with the flow path of between the changed and the unchanged.

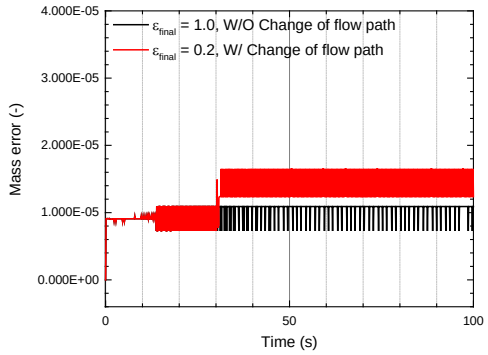

Fig. 3 Comparisons of mass error for the cases between the changed and the unchanged flow path

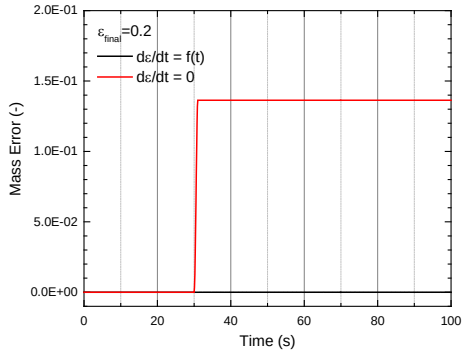

Fig. 4 Comparisons of the effect of porosity change rate on mass error (consideration vs. non-consideration)

Where, $\sum m_{cell,initial}$ is the initial total mass in the pipe, m_{in} and m_{out} is the total mass through the inlet and the outlet during the time from the zero second. $\sum m_{cell}$ is the total mass of pipe at each time and can be written as:

$$\sum m_{\text{cell}} = \sum_{i=1}^{20} \left[\varepsilon_i V_i (\alpha_{g,i}\rho_{g,i} + \alpha_{l,i}\rho_{l,i} + \alpha_{d,i}\rho_{d,i}) \right]$$

V_i and ε_i is the volume and the porosity for each cell, respectively.

From the view of the order of magnitude for mass error, the results between the two cases are reasonable and those values are approximately 10^{-5}. There are a little different trend after the start for changing the flow path. The total mass of pipe is decreased as the flow path is changed from 1.0 to 0.2 after 30 seconds. Therefore, the generation of the difference between the initial total mass and the total mass in the current time step is inevitable due to the change of the porosity.

When the governing equations considering the change of flow path were applied into the SPACE code, it is not only introduced the porosity term to the governing equations, but also the porosity change rate ($\partial\varepsilon / \partial t$) term should be added and considered.

Fig 4 shows the comparison of the mass error when the porosity change rate is not considered and the one when the porosity change rate is not. When the porosity change rate is not considered, the mass error sharply increased according to the change of flow path. These results indirectly reconfirmed that the SPACE code considering the change of flow path is well employed and verified.

4. Conclusions

When ballooning of nuclear fuel generated due to the accidents like as a LBLOCA, the characteristics of mass and heat transfer in a core of nuclear reactor are affected by the change of flow path. The deformation of fuel cladding made a flow in a core detoured or be faster as changing a flow area. These phenomena change instantly. Therefore, it is possible to predict the phenomena by considering the change with time.

In order to analyze these transient phenomena, governing equations considering the change of flow path are employed into the SPACE code by introducing the terms of porosity. The SPACE code is verified with the conceptual problem, which include the change of flow path for single phase flow. Velocities and mass balance are checked and well kept for the change of flow path in single phase flow. The results on the mass balance and the tendency of velocity change are reasonable when compared with no change of flow path case.

Acknowledgement

This work was supported by the Korea Institute of Energy Technology Evaluation and Planning(KETEP) and the Ministry of Trade, Industry & Energy(MOTIE) of the Republic of Korea. (No. 20161510101840)

REFERENCES

[1] A. Prosperetti, S. Sundaresan, S. Pannala, D.Z. Zhang, Segregated methods for two-fluid models, Oak Ridge National Laboratory (ORNL), 2007.